TECHNICAL REPORT RD-RE-90-3

DIFFRACTION PATERN ANALYSIS AS AN OPTICAL INSPECTION TECHNIQUE

Helga A. Alexander
Don Gregory
Research Directorate
Research, Development, and Engineering Center

August 1991

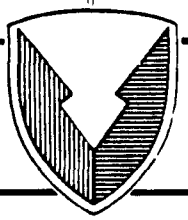

U.S. ARMY MISSILE COMMAND
Redstone Arsenal, Alabama 35898-5000

Approved for public release; distribution is unlimited.

DESTRUCTION NOTICE

FOR CLASSIFIED DOCUMENTS, FOLLOW THE PROCEDURES IN DoD 5200.22-M, INDUSTRIAL SECURITY MANUAL, SECTION II-19 OR DoD 5200.1-R, INFORMATION SECURITY PROGRAM REGULATION, CHAPTER IX. FOR UNCLASSIFIED, LIMITED DOCUMENTS, DESTROY BY ANY METHOD THAT WILL PREVENT DISCLOSURE OF CONTENTS OR RECONSTRUCTION OF THE DOCUMENT.

DISCLAIMER

THE FINDINGS IN THIS REPORT ARE NOT TO BE CONSTRUED AS AN OFFICIAL DEPARTMENT OF THE ARMY POSITION UNLESS SO DESIGNATED BY OTHER AUTHORIZED DOCUMENTS.

TRADE NAMES

USE OF TRADE NAMES OR MANUFACTURERS IN THIS REPORT DOES NOT CONSTITUTE AN OFFICIAL ENDORSEMENT OR APPROVAL OF THE USE OF SUCH COMMERCIAL HARDWARE OR SOFTWARE.

UNCLASSIFIED
SECURITY CLASSIFICATION OF THIS PAGE

REPORT DOCUMENTATION PAGE

Form Approved
OMB No 0704-0188
Exp Date Jun 30 1986

1a. REPORT SECURITY CLASSIFICATION UNCLASSIFIED	1b RESTRICTIVE MARKINGS None
2a SECURITY CLASSIFICATION AUTHORITY N/A	3. DISTRIBUTION / AVAILABILITY OF REPORT Approved for public release; distribution is unlimited.
2b. DECLASSIFICATION / DOWNGRADING SCHEDULE N/A	
4 PERFORMING ORGANIZATION REPORT NUMBER(S) TR-RD-RE-90-3	5. MONITORING ORGANIZATION REPORT NUMBER(S)
6a. NAME OF PERFORMING ORGANIZATION Research Directorate Res., Dev., and Eng. Center 6b. OFFICE SYMBOL (If applicable) AMSMI-RD-RE	7a. NAME OF MONITORING ORGANIZATION
6c. ADDRESS (City, State, and ZIP Code) Commander, U. S. Army Missile Command ATTN: AMSMI-RD-RE-OP Redstone Arsenal, AL 35898-5248	7b. ADDRESS (City, State, and ZIP Code)
8a. NAME OF FUNDING / SPONSORING ORGANIZATION 8b. OFFICE SYMBOL (If applicable)	9 PROCUREMENT INSTRUMENT IDENTIFICATION NUMBER
8c. ADDRESS (City, State, and ZIP Code)	10. SOURCE OF FUNDING NUMBERS PROGRAM ELEMENT NO. / PROJECT NO. / TASK NO. / WORK UNIT ACCESSION NO

11. TITLE (Include Security Classification)
Diffraction Pattern Analysis as an Optical Inspection Technique

12. PERSONAL AUTHOR(S)
Gregory, Don A. and Alexander, Helga A.

13a. TYPE OF REPORT	13b. TIME COVERED	14. DATE OF REPORT (Year, Month, Day)	15. PAGE COUNT
Final	FROM Jun 89 TO Oct 89	August 1991	27

16. SUPPLEMENTARY NOTATION

17. COSATI CODES			18. SUBJECT TERMS (Continue on reverse if necessary and identify by block number)
FIELD	GROUP	SUB-GROUP	Diffraction, Optical inspection

19. ABSTRACT (Continue on reverse if necessary and identify by block number)

A few examples are presented which illustrate the usefulness of optical inspection techniques. Diffraction patterns produced by defects are often distinctive and can be used to examine objects nondestructively. It was also found that if the defect is minor and occupies only a small fraction of the illumination area, the defect diffraction pattern cannot be distinguished from the bright background.

20 DISTRIBUTION / AVAILABILITY OF ABSTRACT	21 ABSTRACT SECURITY CLASSIFICATION
☒ UNCLASSIFIED/UNLIMITED ☐ SAME AS RPT. ☐ DTIC USERS	UNCLASSIFIED
22a. NAME OF RESPONSIBLE INDIVIDUAL Don A. Gregory	22b. TELEPHONE (Include Area Code) (205) 876-7687 / 22c OFFICE SYMBOL AMSMI-RD-RE-OP

DD FORM 1473, 84 MAR 83 APR edition may be used until exhausted
All other editions are obsolete.

SECURITY CLASSIFICATION OF THIS PAGE
UNCLASSIFIED

TABLE OF CONTENTS

LIST OF ILLUSTRATIONS

I. INTRODUCTION

The purpose of this study was to find an optical technique for examining two types of products for manufacturing defects. One of these products was a portion of a metal screen (Fig. 1) commonly used in cathode ray tubes. The CRT screen consisted of a large number of closely spaced rectangular holes with rounded corners. Some of these holes occasionally get blocked during the manufacturing process. This is the kind of defect considered in this investigation. The other type of product under examination was a step–index optical fiber (Fig. 2). Techniques were investigated for checking both the fiber's outer diameter and the core diameter.

Both products were illuminated with light from a Helium- Neon laser. A purposely introduced blockage in the CRT screen was examined by observing the far–field diffraction pattern. In the case of the fiber, the inner and outer fiber diameters were to be determined from the same type of measurement.

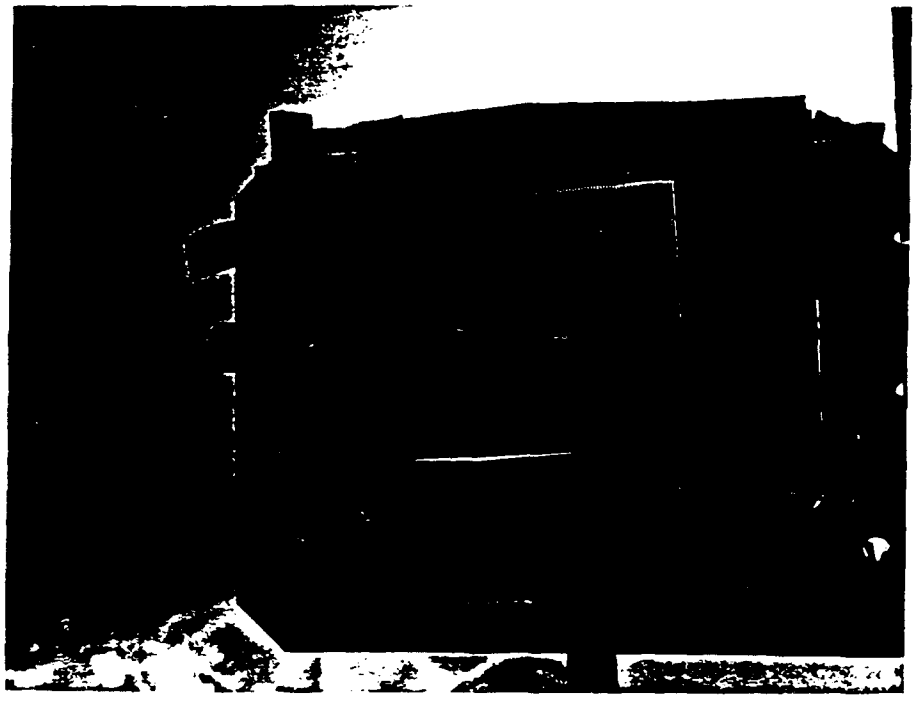

Figure 1. Photograph of the CRT Screen.

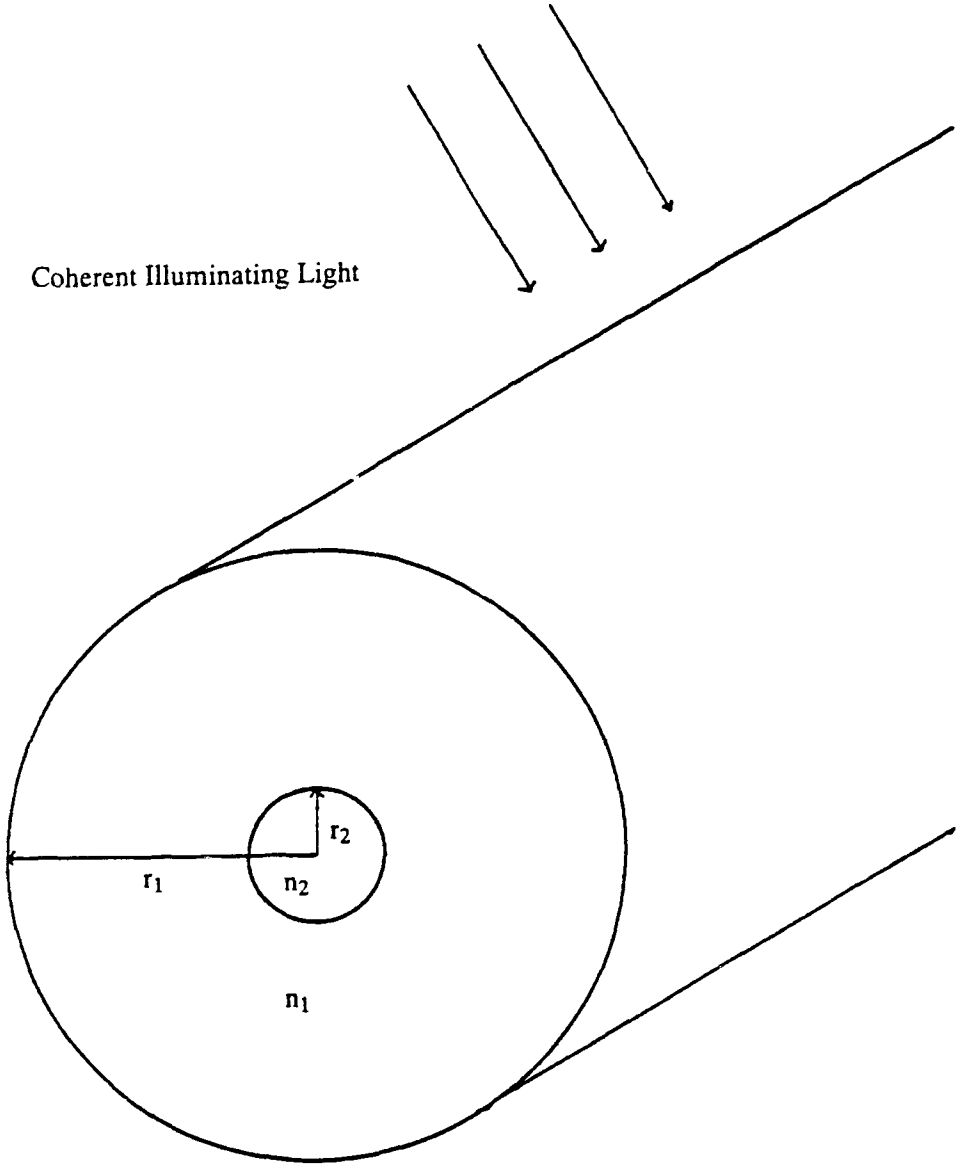

n_1 = 1.4570
n_2 = 1.4624
r_1 = 1.25μm
r_2 = 10μm

Figure 2. Diagram of the Step–index Optical Fiber Studied.

II. BACKGROUND

Diameters of fiber samples have commonly been measured manually with an optical microscope. Marcuse and Presby developed an automatic method for performing these measurements with a microscope [1]. In earlier work, Presby presented a technique for determining the outer fiber diameter by analyzing the back–scattered light when a beam of laser light impinged upon the fiber [2]. Presby and Marcuse extended this back–scattering technique and were able to determine a combination of the refractive indices and the diameters of the core and cladding [3].

Watkins deduced cladding and core diameters from the far–field pattern produced by forward–scattered light [4]. These measurements were performed on fibers with a 19.5 μm core and 166.5 μm cladding diameter, and a .02 refractive index difference between core and cladding. Abushagur and George measured fiber diameters of unclad fibers by taking the Fourier transform of the far–field scattering intensity [5].

Nothing was found in the literature concerning diffraction pattern analysis of a cathode ray tube screen, although treatments of similar apertures are available. The particular CRT screen investigated here is a rather specialized element.

III. GENERAL DIFFRACTION THEORY

Diffraction is the phenomenon of light and dark fringes occurring, when the light path is obstructed, in areas which should be (according to principles of geometrical optics) uniform shadow regions. Diffraction can be analyzed using the Huygens–Fresnel principle, which states that "every unobstructed point of a wavefront, at a given instant in time, serves as a source of spherical secondary wavelets [6]". Diffraction is, thus, a consequence of the superinpositioning of waves.

Diffraction effects are generally classified into two types. Fresnel (or near–field) diffraction occurs when both the plane of observation and the point source of illuminating light are relatively close to the diffracting aperature, so that the waves impinging on the aperture as well as those arriving at the observation screen are spherical. The diffraction pattern changes significantly when the distance to the screen is slightly increased or decreased. Fraunhofer (or far–field) diffraction occurs when the wave fronts impinging on and leaving the diffracting aperture approach being planar. This can be achieved either with the aid of lenses or by positioning the illuminating point source and screen far from the aperture. Moving the screen under these conditions will change the size but not the shape of the diffraction pattern. Only far–field diffraction effects were examined in this investigation.

The far–field diffraction pattern observed depends on the size and shape of the diffracting aperture. The irradiance distribution of a uniformly illuminated single slit aperture is given by [6] :

$$I(\theta) = I(O) (\sin \beta/\beta)^2$$

where

$$\beta = (kb/2) \sin \theta$$

and $k = 2\pi/\lambda$, λ is the wavelength of the light, b is the width of the slit, θ is the angular deviation from the central maximum, and I(O) is the peak irradiance (Fig. 3). This shows that the irradiance falls off rapidly as θ increases, so that the higher order maxima in the diffraction pattern are relatively dim compared to the brightness of the central order.

The condition for diffraction minima can be derived from the above expression for the irradiance distribution.The first diffraction minimum thus occurs when:

$$b \sin \theta = \lambda.$$

For small θ,

$$\sin \theta = x/f,$$

where x is the distance from the central order to the center of the first dark order, and f is the focal length of the transform lens. Hence, the distance to the first minimum can be calculated when the slit width is given:

$$x = \lambda f/b,$$

or the slit width can be computed by measuring the distance to the first minimum of the diffraction pattern.

A stop, which is complementary to a single slit, i.e., a long narrow opaque obstacle (such as a thin wire or hair) will produce a diffraction pattern identical to that of a single slit. This is known as Babinet's principle [6]. Therefore, the equations discussed above, in connection with the single slit, can also be used to determine the width of such an obstruction.

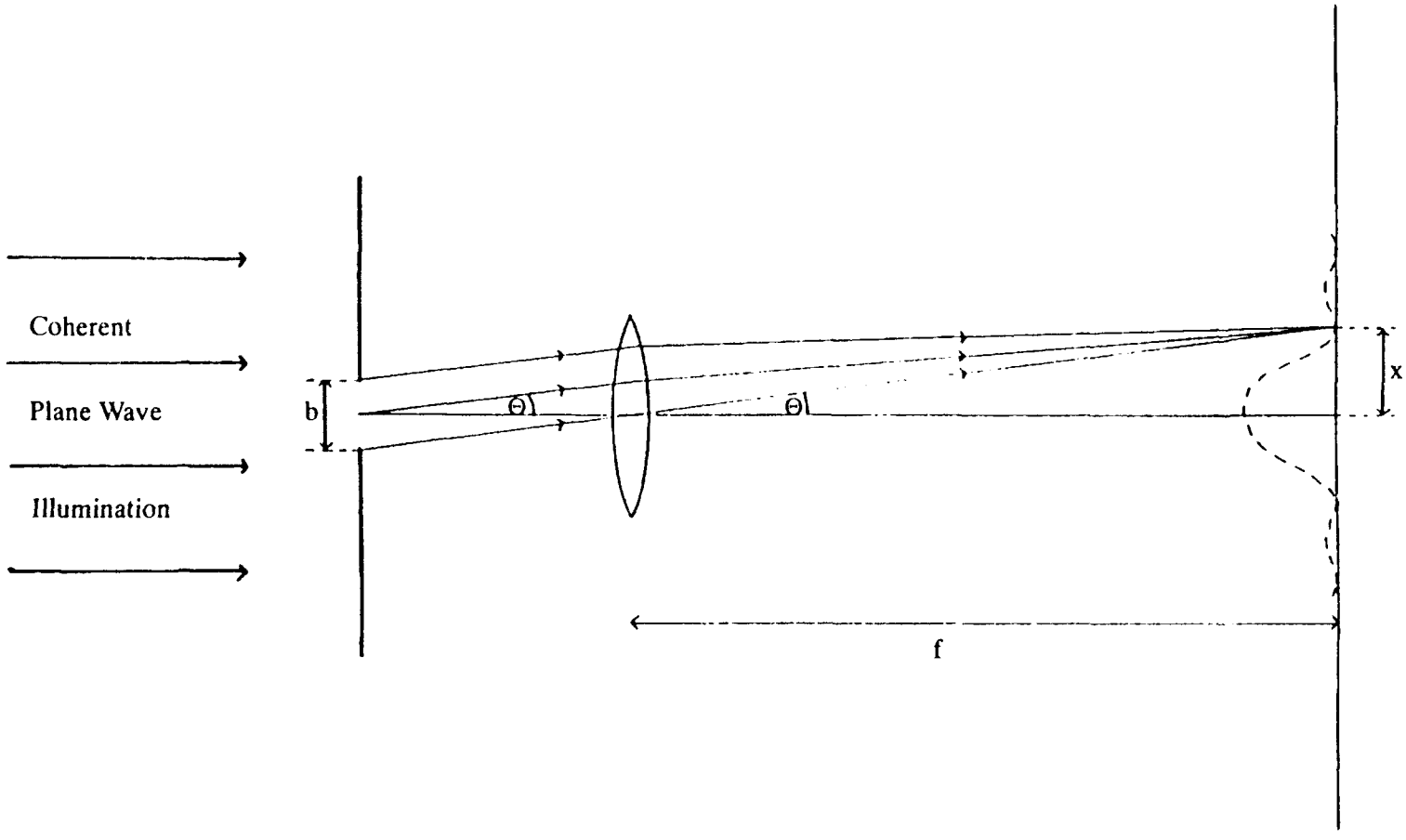

Figure 3. Fraunhofer Diffraction of a Single Slit Illuminated by Monochromatic Plane Waves.

IV. THEORY AS APPLIED TO THE PROBLEM

A. Fiber

A transversely illuminated glass fiber, with or without an inner core, represents a more complicated aperture than a single slit or a long thin opaque obstruction. However, it has the shape of such an aperture and produces a diffraction pattern which, to some extent, depends only on the outside diameter of the fiber. In addition to this, light is also transmitted, refracted and reflected by the fiber, which can add coherently to the diffracted light and result in a composite far–field pattern [4].

According to Watkins, there is a range of angles for which two transmitted rays may leave the fiber at the same scattering angle and thus interfere. One of these rays passes through the cladding only, the other through the cladding and the core. Figure 4 shows that there is a critical angle θc which defines the lower limit of this range. It is the scattering angle of the ray just grazing the core. All pure cladding rays will experience a scattering angle larger than θc. (According to Watkins) :

$$\theta c = 2\,[\arcsin(n_1 r_2/r_1) - \arcsin(r_2/r_1)].$$

This equation gives a computed value of 4.21° for the fiber investigated here.

There is no contribution from cladding rays or from reflected rays at scattering angles smaller than θc. In this range, the far–field pattern is due to diffraction effects caused by the outer fiber diameter plus light transmitted through the core of the fiber. As mentioned before, a single slit diffraction pattern has most of its energy in and close to the central order. Since θc is small, the effects of diffraction can be expected to dominate the pattern in this region, although the transmitted rays may cause a slight modulation.

Above this critical scattering angle, interference between reflected rays, pure cladding rays, and core rays should dominate the far–field pattern, causing it to differ in appearance from the pattern in the 0° to θc range. Thus, an experimental value for θc should be observable, which can be used, together with the experimental value for the outer diameter (determined from the distance to the first dark fringe) in the equation for θc given by Watkins to compute a value for the core diameter.

B. CRT Screen

Figure 5 shows micrographs of individual openings in the CRT screen. The overall pattern can be seen more clearly in Fig. 6. When the screen is illuminated with collimated laser light, it produces the Fraunhofer pattern depicted in Fig. 7. Using the distance from the principal maximum to the first minimum in the equation for the single slit discussed in Section III, the width of the individual openings can be computed. In fact, most of the features of the diffraction pattern can be related to their corresponding distances on the CRT screen by using the single slit approximation.

Further fine structure details are revealed when the diffraction pattern is magnified. Figure 8 is a photograph of the magnified pattern displayed on a television monitor. What appear to be primary orders in this photograph are in fact the secondary orders seen in Fig. 7. Masking out some of these bright spots enhanced the visibility of another set of subsidiary orders in the horizontal and vertical directions. This set of subsidiary orders is due to diffraction from the square iris.

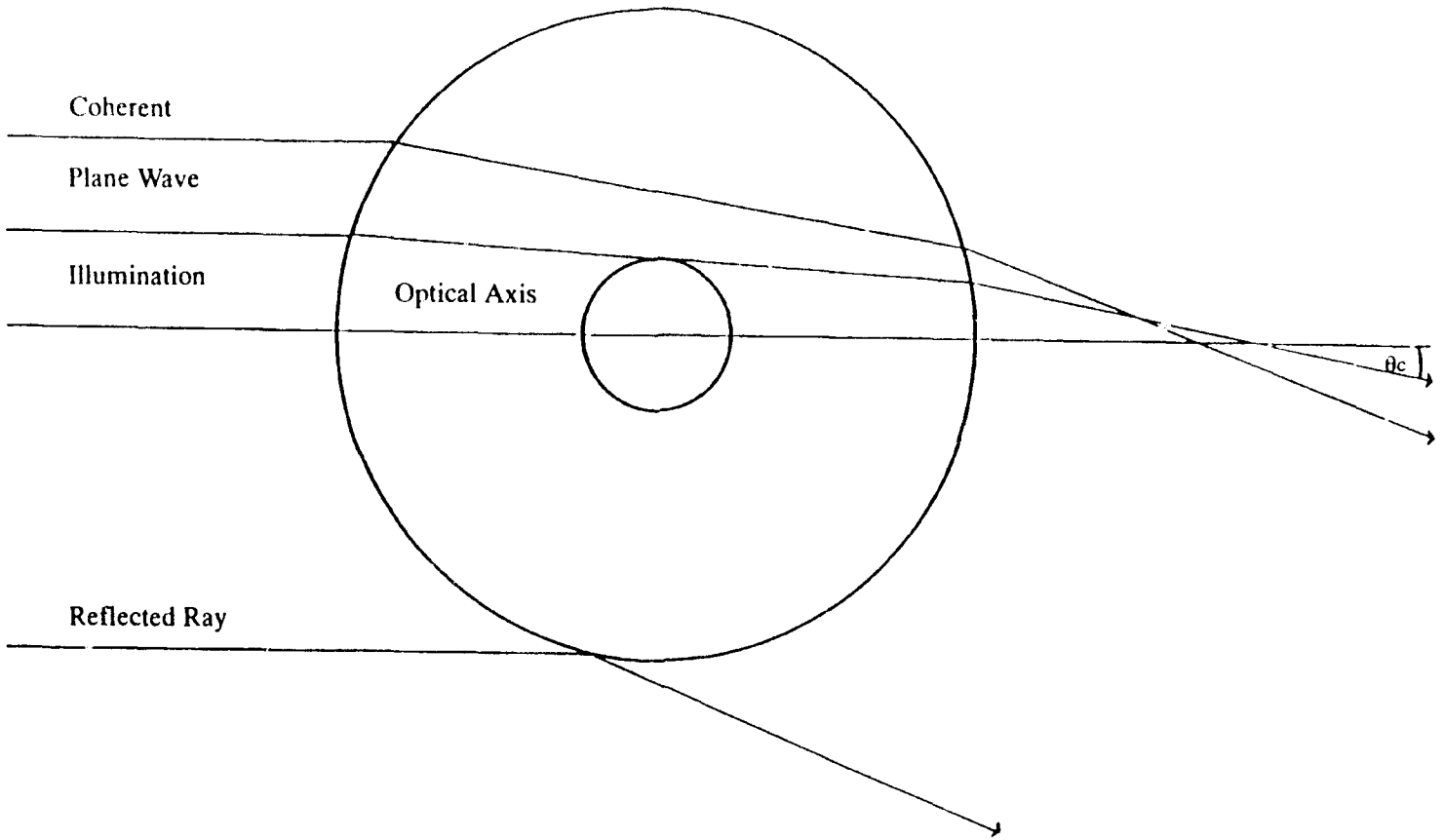

Figure 4. Cross-section of Fiber Which Shows the Critical Scattering Angle θ_c Defined by the Refracted Ray Just Grazing the Core. All Other Pure Cladding Rays are Scattered at an Angle Larger than θ_c. Also Shown is a Reflected Ray.

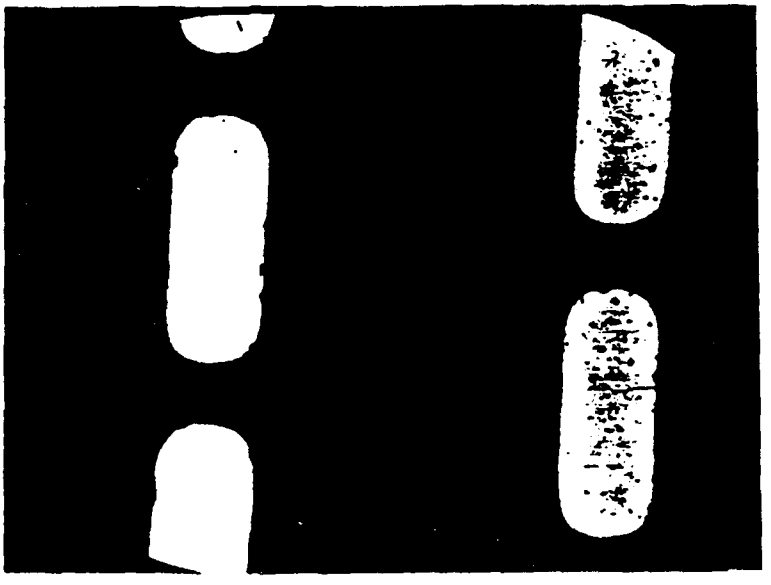

Figure 5. Micrographs of an Individual Opening (100x Magnification) and of Several Openings (50x Magnification) in the CRT Screen.

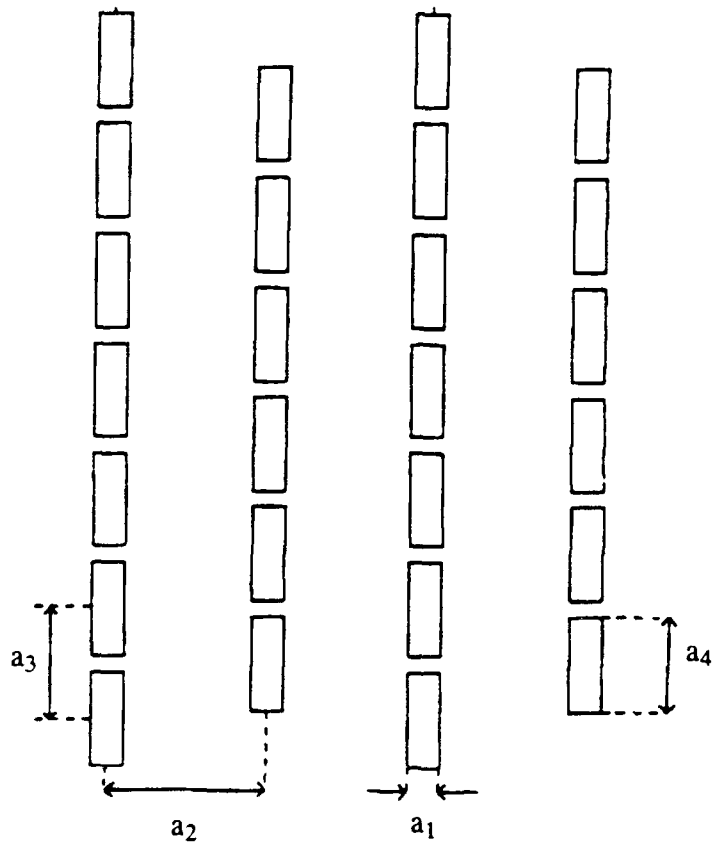

Figure 6. Hole Pattern of the CRT Screen.

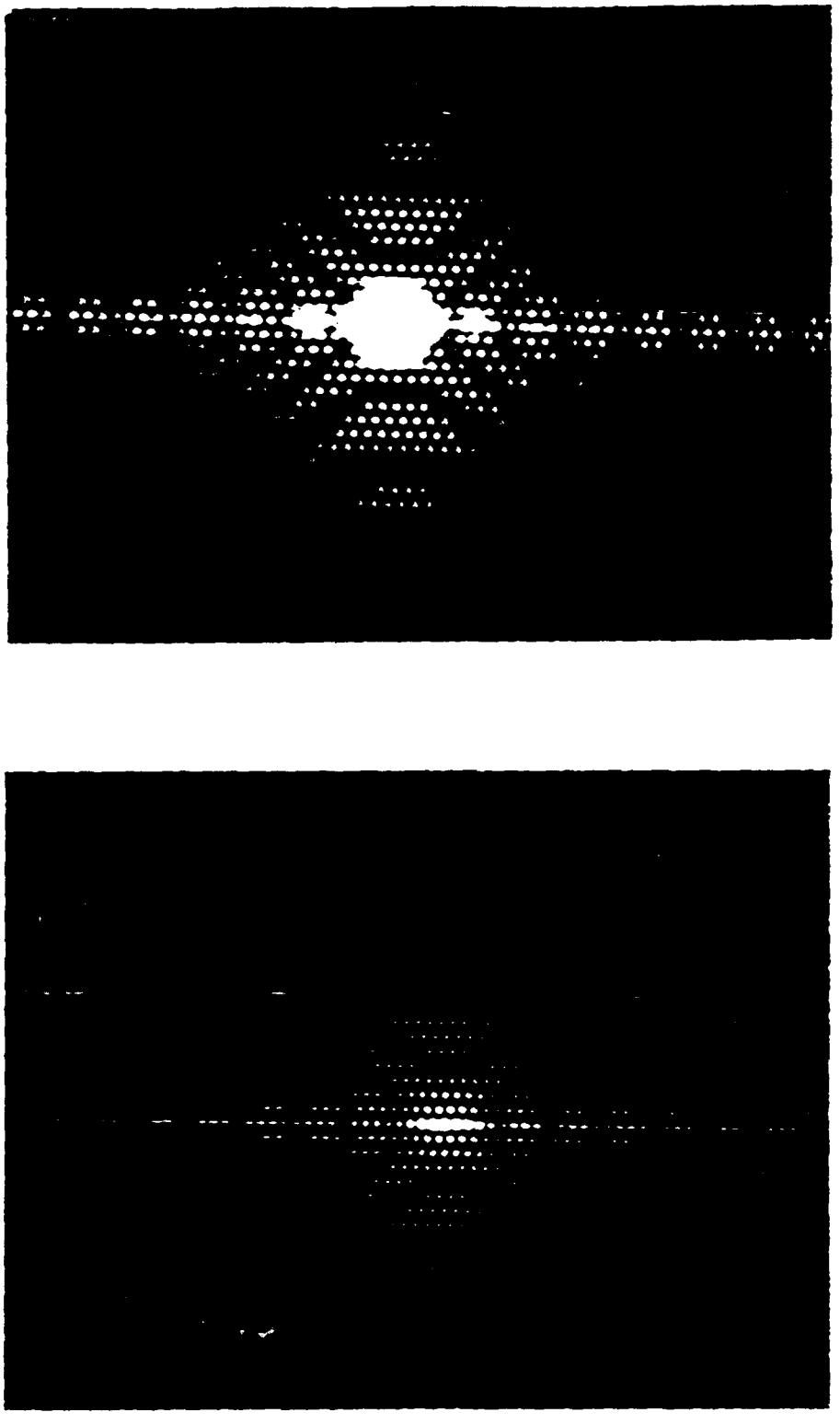

Figure 7. Photographs, Using Different Exposures, of the Far–field Diffraction Pattern Produced by the CRT Screen.

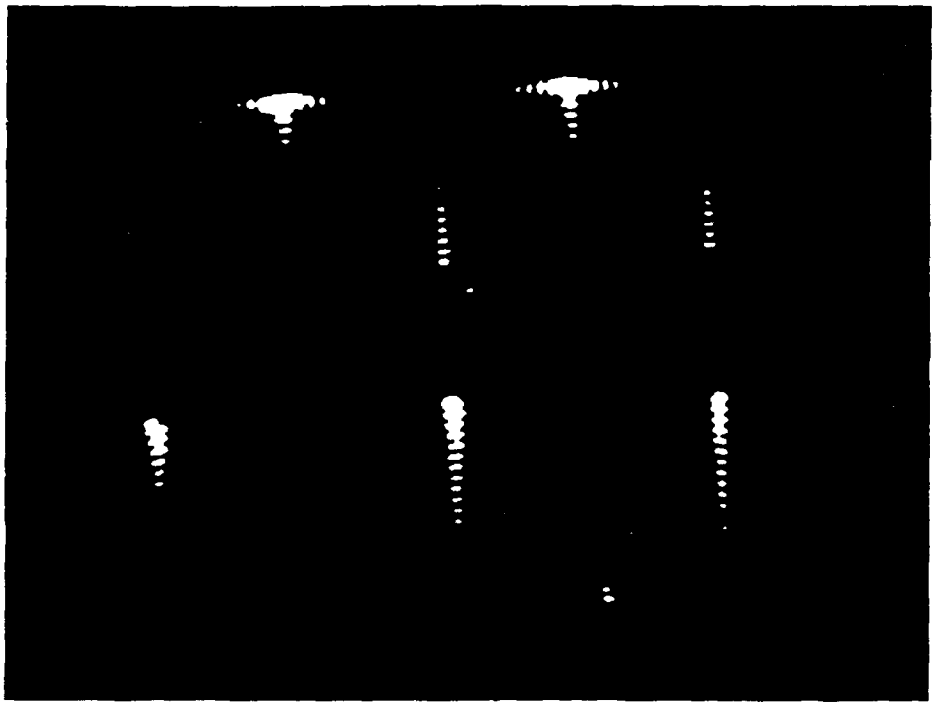

Figure 8. Photograph of the Magnified Diffraction Pattern of the CRT Screen Displayed on a TV Monitor.

V. EXPERIMENTAL ARRANGEMENT AND RESULTS

A. Fiber

Figure 9 is a schematic drawing of the experimental set–up used for the fiber study. A 4 mW Uniphase Model 1107P Heli· ¬–Neon laser was used, which produced a reasonably well collimated beam of 3 mm diameter. This beam was incident perpendicular to the long axis of the optical fiber. The fiber illuminated was specified as having a cladding diameter of 125 μm and a core diameter of 10 μm. The index of refraction of the cladding was given a 1.4570, that of the core as 1.4624. Figure 10 is a photograph of the fringe pattern observed on a white cardboard screen located one focal length (2.28 m) behind the transform lens. Black tape was used to cover part of the bright central order and absorb some of the glare. Many more fringes could be seen on the screen than it was possible to capture in the photograph. The diffraction pattern obtained was similar to that of a single slit aperture. The distance to the first minimum was measured to be 1.1 ± .05 cm. Using this value in the equation for computing the slit width as outlined in a previous section, a corresponding slit width of 131.2 μm was calculated. Assuming the specified value of 125 μm to be correct, measuring the distance to the first diffraction minimum determined the outer diameter of the fiber to within an accuracy of 5%.

At a distance of approximately 15 cm from the central order, a change in the pattern was observed. The fringes were not so well defined, and the dark fringes were not as distinctly dark as they were at a closer distance to the central order. Hence, this was taken as the distance on the screen corresponding to the critical angle θc, above which interference between pure cladding, core, and reflected rays should dominate the pattern. The corresponding critical angle θc was computed to have a value of 3.77°. This value is 10% lower than the critical value computed by using the real fiber diameters. Having found an experimental value for θc and for the outer radius r_1, the core diameter could be computed from the equation for θc by an iteration method. The value thus found for the inner core diameter was 9.4 μm, 6% lower than the specified value.

B. CRT Screen

Figure 11 depicts one of the experimental arrangements used for the CRT screen study. A collimated beam from a 35 mW Spectra–Physics Model 124B Helium–Neon laser was incident normally on the CRT screen. The screen was oriented such that the short sides of the rectangular openings were parallel to the optical table. A 2.28 m transform lens was used to focus the far–field diffraction pattern on a white cardboard screen. Figure 7 shows photographs of the pattern observed with this experimental set–up. One of the photographs was given a longer exposure time to enhance the visibility of the higher orders.

The distance between the principal orders in the horizontal direction was measured to be 6.5 ± 0.5 mm. Using the single slit approximation discussed in Section III, one obtains a corresponding "slit" width of 0.22 mm. This is in very good agreement with a value of 0.215 ± .005 mm for the width of an opening in the screen (distance a_1 in Fig.6) measured from the micrograph. Similarly, the measured distance of 1.5 ± .1 mm between the subsidiary maxima in the horizontal direction gives a value of .96 mm for the horizontal center to center spacing (a_2 in Fig. 6) of the screen openings, which agrees well with the value of .98 ± .01 mm obtained from the micrograph.

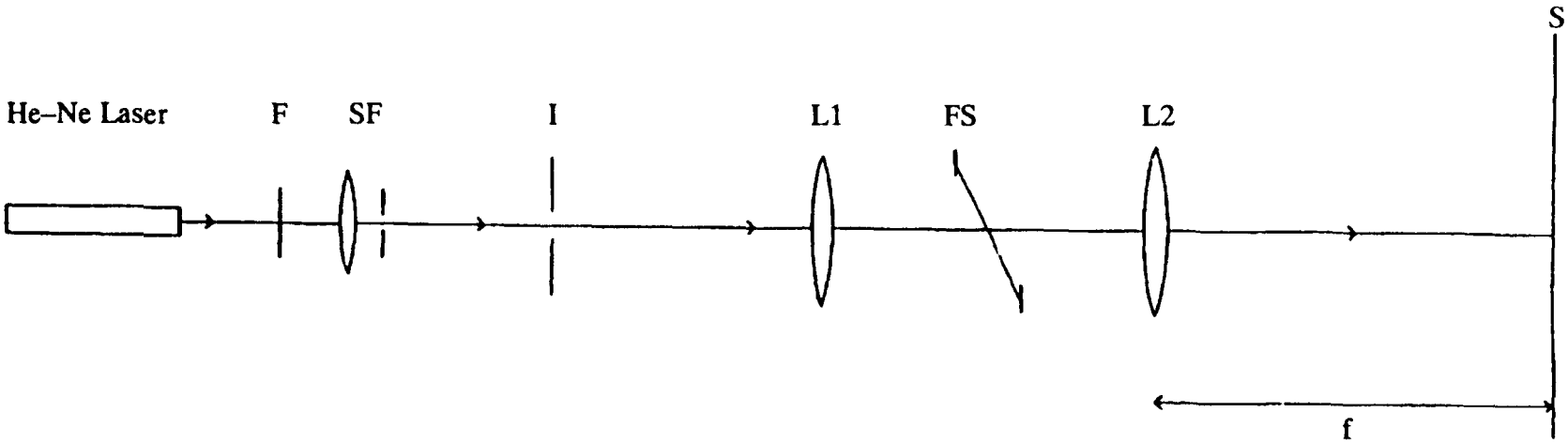

F– Neutral–density Filter
SF – Spatial Filter
I – Iris
L1 – Collimating Lens
FS – Fiber Sample
L2 – Transform Lens
S – Cardboard Screen

Figure 9. Experimental Arrangement Used for the Fiber Study.

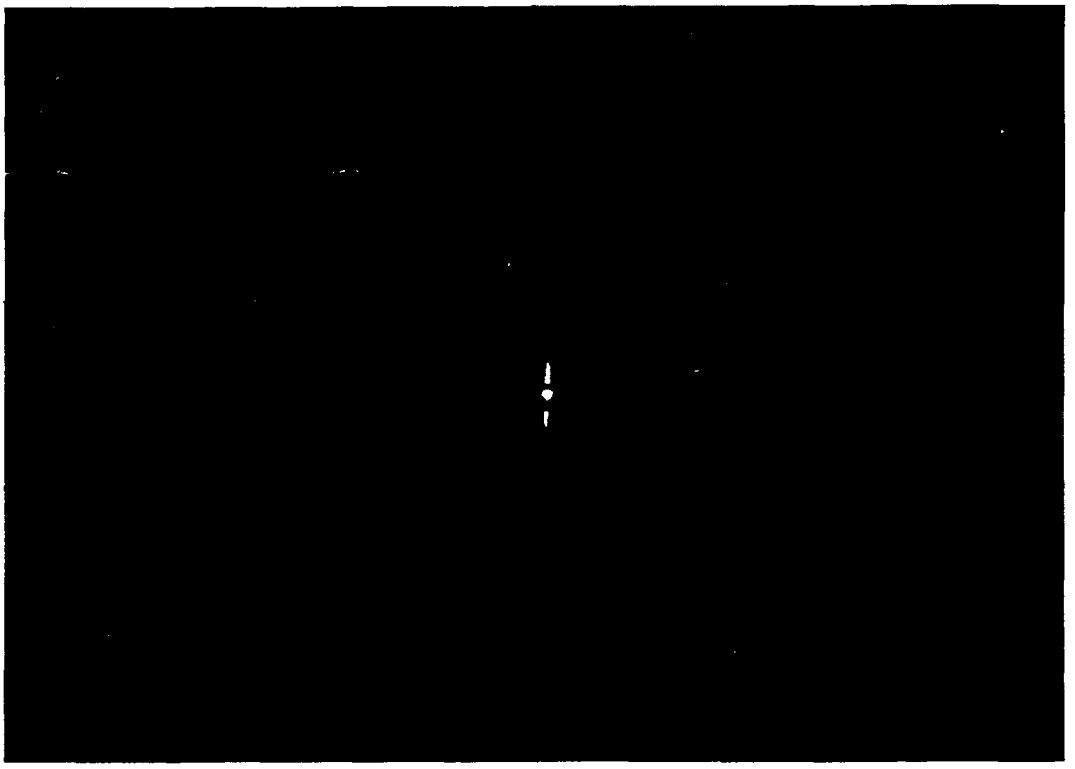

Figure 10. Photograph of the Far–field Diffraction Pattern Produced by the Fiber.

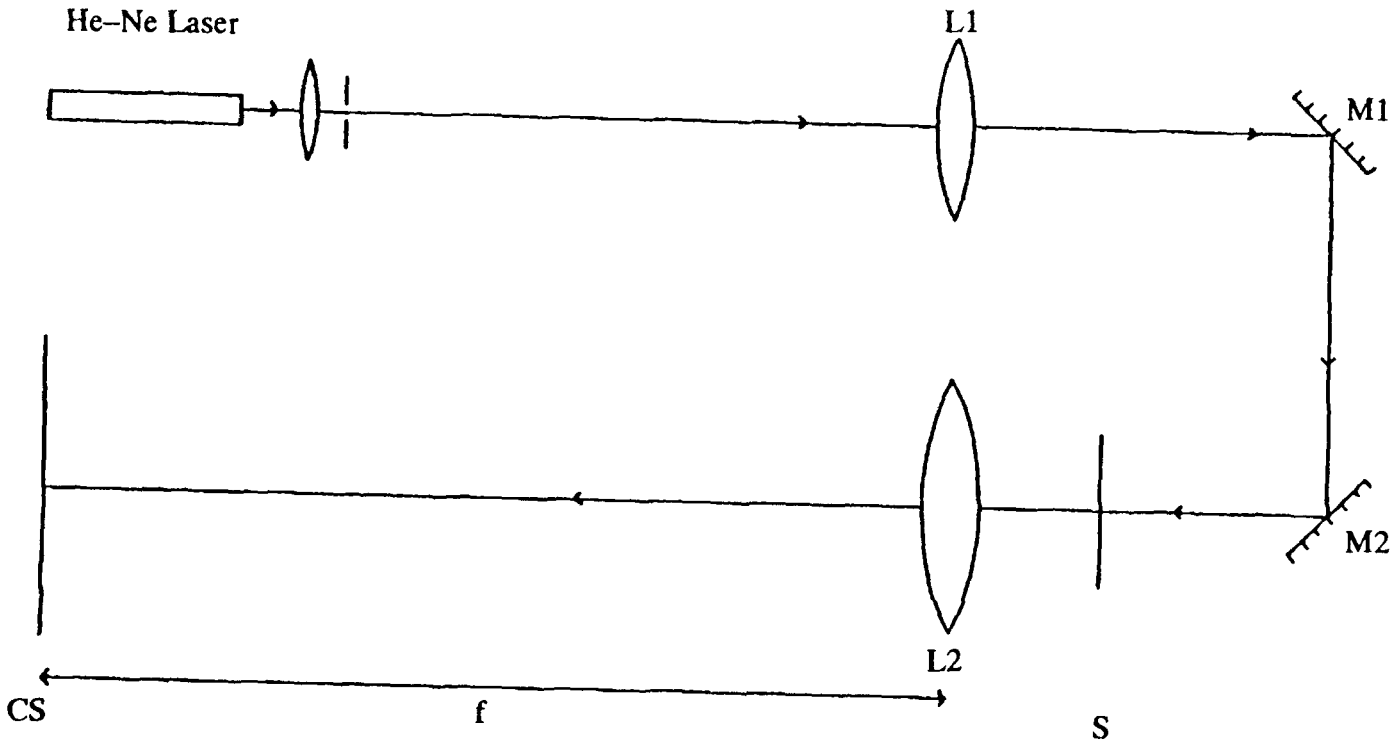

SF	–	Spatial Filter	S	–	CRT Screen
L1	–	Collimating Lens	L2	–	Transform Lens
M1, M2	–	Mirrors	CS	–	Cardboard Screen

Figure 11. Experimental Arrangement Used to Observe the Diffraction Pattern of the CRT Screen on a Cardboard Screen.

The distance between the subsidiary maxima in the vertical direction was measured to be 2.0 ± .1 mm. This corresponds to an aperture distance of .72 mm. The vertical center to center spacing between the screen openings was measured to be .80 ± .01 mm, while the slit height was .65 ± .1 mm (a_3 and a_4, respectively, in Fig. 6). It is thus difficult to determine which of these two dimensions in the CRT screen causes the 2 mm spacing between the subsidiary maxima in the vertical direction. The chevron features of the diffraction pattern are most likely due to the slightly rounded structure of the slits.

No change in the pattern was visible when a small blockage was introduced into the CRT screen. Therefore, the diffraction pattern had to be magnified to observe some of the finer structure. The experimental arrangement was changed to that depicted in Fig. 12. A magnification factor of 15.75 was achieved using an RCA television camera and displaying the diffraction pattern on a television monitor. Changing the 2.28 m transform lens to a lens combination with an effective focal length of 5.58 m provided further magnification. A 4 mW Uniphase Helium–Neon laser was used because the sensitivity of the television camera required a much lower light intensity.

A square–shaped iris gave the collimated laser beam incident on the CRT screen a square cross–section of 1.9 cm by 1.9 cm. It was found that the effects of introducing a small blockage in the screen were less noticeable in the diffraction pattern when a beam of circular cross–section was used. The square beam illuminated approximately 650 openings in the screen.

Figure 8 is a photograph of the far–field pattern displayed on the screen, after black tape was placed across the TV camera to block out the brightest orders. The bright orders in this photograph are, in fact, the secondary orders seen in Fig. 7. The additional subsidiary orders visible with this experimental arrangement are due to diffraction from the square iris. A square beam of 1.9 cm by 1.9 cm should produce diffraction orders in both the horizontal and vertical direction located a distance of 2.9 mm apart on the TV monitor. The actual distance measured was 3.0 ± .5 mm.

Upon introduction of a blockage covering one hole of the CRT screen, no change was observed in the far–field pattern. However, when the blockage was enlarged to cover five of the 650 openings illuminated, a remarkable change in the subsidiary orders of the resulting diffraction pattern was observed. Figures 13a and 13b show the pattern without the blockage and with the blockage in place, respectively. Additional bright orders had to be masked to increase the visibility of the subsidiary orders. When the blockage was in the center of the illuminated screen area, every other subsidiary maximum seemed to be enhanced, while the maxima previously visible between the enhanced ones disappeared. This effect was no longer visible when a larger area of the screen was illuminated

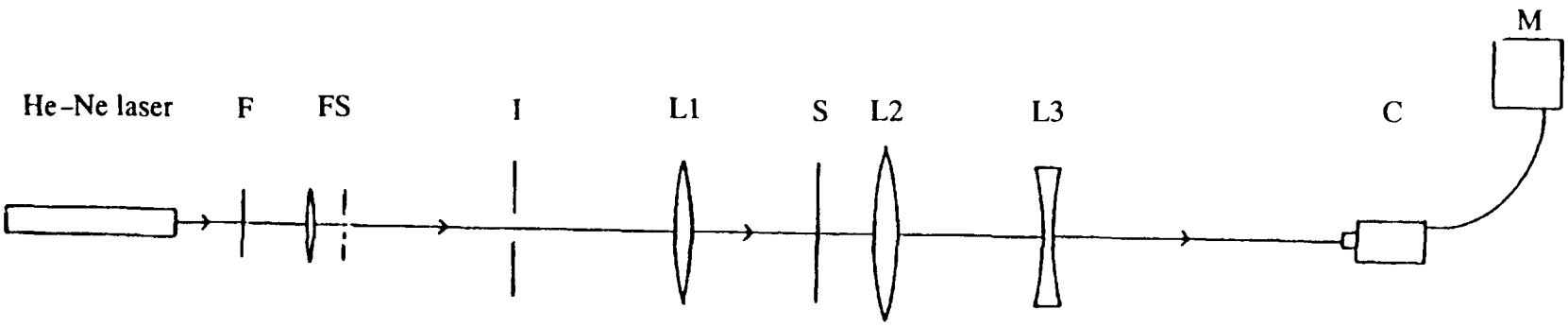

F – Neutral Density filter
SF – Spatial Filter
I – Iris
L1 – Collimating Lens
S – CRT Screen
L2, L3 – Transform Lens System
C – TV Camera
M – Monitor

Figure 12. Experimental Arrangement Used to Observe the Diffraction Pattern of the CRT Screen on a TV Monitor.

Figure 13a. Photograph of the CRT Screen's Diffraction Pattern Showing Some of the Subsitiary Orders When No Blockage is Present.

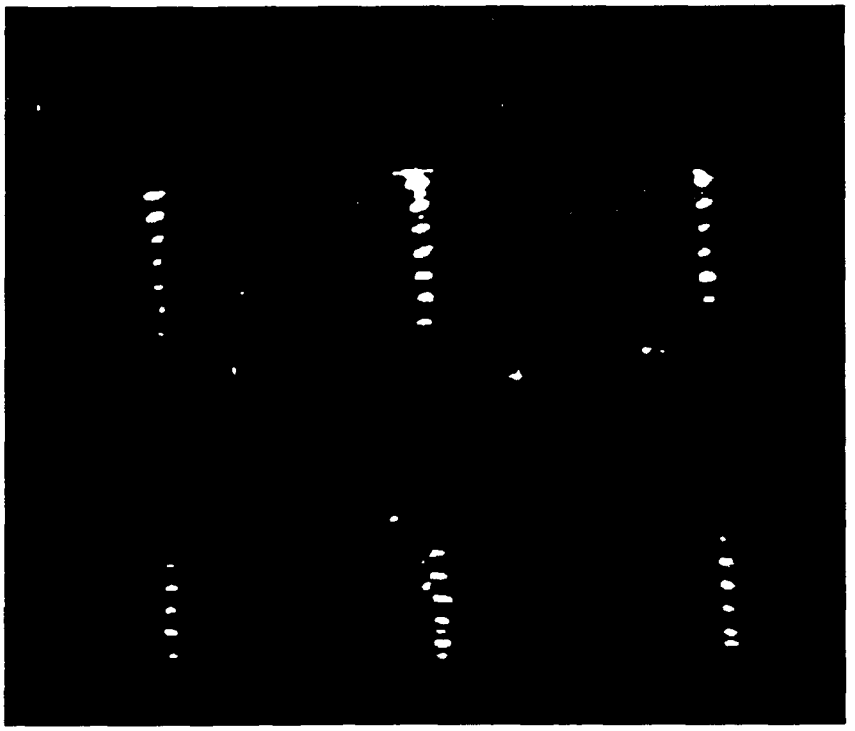

Figure 13b. Photograph of the CRT Screen's Diffraction Pattern When a Blockage is Introduced.

VI. DISCUSSION OF RESULTS

A. Fiber

The accuracy with which the cladding and core diameters were determined in this investigation could be greatly improved in future studies. The outer diameter values were based on a single–slit approximation. It did not take into account the transparency and difference in geometry of a circular–cylindrical fiber as compared to a thin flat totally absorbing strip. It would be useful to compare the diffraction pattern of the fiber to that of an actual slit with a slit width equal to the outer fiber diameter, in order to determine the percentage error introduced by this approximation. Such a calculation was performed by Greenler et al. for transparent cylinders with indices of refraction varying between 1.4 and 1.5 [7]. It showed that the errors introduced by the single–slit approximation ranged from 33% to 47% for cylinders of 5.5 μm diameter. Fibers of diameters comparable to the one examined in this investigation were not considered by Greenler et al. They claim, however, that the error would still be considerable for a transparent cylinder with a diameter larger than 5.5 μm

Another source of error lies in the measurement of the distance to the first dark fringe, followed by the approximation $\sin \theta = x/f$. Use of a detector capable of measuring the intensity of the scattered light at the actual scattering angles would make the outer diameter determination more accurate, since the scattering angle at which the intensity is at a minimum could more easily be detected on a graph of intensity versus scattering angle. Such a graph should also make determination of the critical scattering angle θc more accurate, thus improving the accuracy with which the core diameter can be computed. In this study, the scattering angle θc was found by making a visual judgement as to where the diffraction pattern on the screen changed. This judgement could probably be made with more certainty from a graph of the angular distribution of the scattered light, thus diminishing this source of error.

Considering the many possibilities for error, the relatively small discrepancies between the experimentally determined and true fiber diameters may be the result of some errors partially cancelling each other.

B. CRT Screen

The actual pattern of the openings in the CRT screen is obviously much more complex than a single slit aperture. Nevertheless, it was shown that the single slit approximation can be used to satisfactorily relate many features of the diffraction pattern to the corresponding parts of the CRT screen.

Blocking some of the openings in the screen led to a change in that part of the diffraction pattern which was originally due to diffraction from the square iris. Interference due to the blockage and the square aperture thus caused some of these subsidiary maxima to be enhanced,while others disappeared. However, an exact analysis of this phenomenon is beyond the scope of this investigation.

VII. CONCLUSION

A. Fiber

The outer diameter of a step–index fiber was determined with an accuracy of 5% by measuring the distance to the first dark fringe in the far–field diffraction pattern. A value for the core diameter was then found based on the experimental value for θc. This represents the scattering angle of a cladding ray grazing the core (Fig.4). In the scattering range below θc, interference effects between pure cladding rays, core rays, and reflected rays are not possible. An equation developed by Watkins [4] was utilized to compute the core diameter. The computed core diameter differed from the one specified by 6%. This study differs from that by Watkins in that the scattering region below θc was used to determine the outer diameter.

The difference in index refraction between core and cladding of the fiber used in this investigation was only 0.0054, compared to an index difference of 0.02 in the fiber studied by Watkins. The fiber investigated also had much smaller inner core diameter than fibers studied in previous work of other authors. Future investigations could achieve better results with a slightly more sophisticated experimental set–up than the one used in this study.

B. CRT Screen

A blockage covering five openings of the CRT screen examined was found to cause a detectable change in the screen's far–field diffraction pattern. No such change was observed when the blockage was reduced in size or when the area illuminated was increased to cover more than approximately 650 openings. Hence, this technique would have to be improved further in order to become a feasible method for detecting a small number of blocked openings in CRT screens.

REFERENCES

1. Marcuse, D. and Presby, H. M., Applied Optics, Vol. 18, pp. 402–408, 1979.

2. Presby, H. M., Journal of the Optical Society of America, Vol. 64, pp. 280–284, 1974.

3. Presby, H. M. and Marcuse, D., Applied Optics, Vol. 13 pp. 2882–2885, 1974.

4. Watkins, L. S., Journal of the Optical Society of America, Vol. 64, pp. 767–772, 1974.

5. Abushagur, M. A. G. and George, N., Applied Optics, Vol. 19, pp. 2031–2033, 1980 .

6. Hecht, E., Optics, 2nd Edt., Addison–Wesley, Reading, MA, 1987.

7. Greenler, R. G., Hable, J. W. and Slane, P. O., "Diffraction around a fine wire: How good is the single–slit approximation?", in press, American Journal of Physics.

DISTRIBUTION LIST

	Copies
AMSMI–RD	1
AMSMI–RD–CS–R	15
AMSMI–RD–CS–T	1
AMSMI–GC–IP, Mr. Fred M. Bush	1
U. S. Army Materiel System Analysis Activity ATTN: AMXSY–MP (Herbert Cohen) Aberdeen Proving Ground, MD 21005	1
IIT Research Institute ATTN: GACIAC 10 W. 35th Street Chicago, IL 60616	1
Director U.S. Army Research Office ATTN: SLCRO–PH ATTN: SLCRO–ZC P. 0. Box 12211 Research Triangle Park, NC 27709–2211	1
Headquarters Department of the Army DAMA–ARR Washington, D.C. 20310–0632	1
Headquarters OUSDR&E The Pentagon ATTN: Dr. Ted Berlincourt Washington, D.C. 20310–0632	1
Defense Advanced Research Projects Agency Defense Sciences Office Electronics Systems Division ATTN: Andy Tang 1400 Wilson Boulevard Arlington, VA 22209	1
Commander U.S. Army Foreign Science and Technology Center ATTN: AIAST–RA 220 Seventh Street, NE Charlottesville, VA 22901–5396	1

	Copies
Director, URI University of Rochester College of Engineering and Applied Science The Institute of Optics Rochester, NY 14627	1
Director, JSOP University of Arizona Optical Science Center Tucson, AZ 85721	1
Electro–Optical Terminal Guidance Branch Armament Laboratory ATTN: Dr. Steve Butler Eglin Air Force Base, FL 32542	1
U. S. Army CRREL ATTN: Dr. Richard Munis 72 Lyme Mill Road Hanover, NH 03755	1
Night Vision and Electro–Optics Center ATTN: AMSEL–NV–T/Mark Norton Building 357 Fort Belvoir, VA 22060	1
RADC/ESOP ATTN: Dr. Joseph Horner Hanscom AFB, MA 01731	1
Applied Science Division Applied Optics Operations ATTN: Dr. George Keene P. O. Box 3115 Garden Grove, CA 92641	1
Department of Electrical Engineering Standford University ATTN: Dr. J. W. Goodman Standford, CA 94305	1
University of Alabama in Huntsville Center for Applied Optics ATTN: Dr. H. John Caulfield Huntsville, AL 35899	1
University of Alabama in Huntsville Physics Department ATTN: Dr. J. G. Duthie Huntsville, AL 35899	1

	Copies
Carnegie–Mellon University Department of Electrical and Computer Engineering ATTN: Dr. David Casasent Pittsburgh, PA 15213	1
The Pennsylvania University Department of Electrical Engineering ATTN: Dr. F. T. S. Yin University Park, PA 16802	
University of Alabama in Birmingham Physics Department ATTN: Mr. James F. Hawk University Station Birmingham, AL 35294 NASA	1
Johnson Space Center ATTN: Code EE–6, Dr. Richard Juday Houston, TX 77058	1
Jet Propulsion Laboratory ATTN: Dr. Michael Shumate 4800 Oak Grove Drive Pasadena, CA 91109	1
Naval Weapons Center ATTN: Code 3941, David Bloom China Lake, CA 93555	1
University of Colorado at Boulder Department of Electrical and Computer Engineering ATTN: Dr. Kristina Johnson Boulder, CO 80309–0425	1
Naval Research Laboratory ATTN: Code 6537, Dr. Arthur Fisher Washington, D.C. 20375–5000	1
AMSMI–RD–RE, Dr. J. Bennett	1
AMSMI–RD–RE–OP, Dr. Don A. Gregory	80
AMSMI–GC–IP	1
DASD–H–V	1